Distributions of Phytoplankton Blooms in the Southern Ocean

C. W. Sullivan,* K. R. Arrigo, C. R. McClain, J. C. Comiso, J. Firestone

A regional pigment retrieval algorithm for the Nimbus-7 Coastal Zone Color Scanner (CZCS) has been tested for the Southern Ocean. The pigment concentrations estimated with this algorithm agree to within 5 percent with in situ values and are more than twice as high as those previously reported. The CZCS data also revealed an asymmetric distribution of enhanced pigments in the waters surrounding Antarctica; in contrast, most surface geophysical properties are symmetrically distributed. The asymmetry is coherent with circumpolar current patterns and the availability of silicic acid in surface waters. Intense blooms (>1 milligram of pigment per cubic meter) that occur downcurrent from continental masses result from dissolved trace elements such as iron derived from shelf sediments and glacial melt.

Knowledge of global-scale features of phytoplankton biomass and productivity is crucial to the understanding of the role of the Southern Ocean [ocean area south of 30°S latitude (*1*)] in the contemporary global carbon cycle of matter (*2–5*) and the relation between the distributions of primary producers and higher trophic-level consumers on a planetary scale. Phytoplankton are the major agents in the sea responsible for the transformation of about 50×10^{15} g of carbon dioxide annually into fixed organic carbon (phytoplankton biomass) (*6, 7*). These single celled plants represent a major potential sink for atmospheric carbon dioxide in the sea (*6, 8*) as well as the major source of carbon and energy for the oceanic food web (*9*). Accurate assessments of large-scale phytoplankton distribution, abundance, productivity, and sedimentation rates are difficult to obtain by conventional ship-based studies with their characteristic low spatial and temporal resolution. This problem is especially true for the Southern Ocean, where severe weather and sea ice greatly restrict ship access (*10–12*).

Satellite data can be an important source of ocean basin–scale pigment distributions and standing crop estimates at high latitudes, but adequate validation is necessary because of uncertainty associated with low sun angles, multiple scattering effects, and unknown bio-optical characteristics of surface waters. Blooms in several areas of the Southern Ocean have been reported previously; however, spatial distributions of these blooms were relatively unknown until the advent of the Nimbus-7 CZCS. The CZCS pigment data are useful for the characterization of large-scale surface features of the Southern Ocean (*12, 13*). Previous quantitative comparisons of in situ pigments [chlorophyll *a* and phaeopigments (chl *a* + phaeo)] with the current CZCS algorithm (*14*) have been encouraging. However, these studies either made use of small Southern Ocean data sets that were spatially restricted (*10, 11*) or focused on the northern hemisphere (*15*). In this article, we examine the validity of the satellite-derived pigment distributions in the Southern Ocean by comparing historical pigment concentrations from CZCS with in situ measurements from around the Southern Ocean. We also discuss qualitative and quantitative aspects of the bloom patterns in relation to geophysical and ecological features of the Southern Ocean.

Comparison of Satellite with in Situ Pigment Data

We compared average summer in situ pigment concentrations collected from ships from waters south of 30°S latitude with CZCS climatologies averaged over relevant temporal and spatial scales to assess the applicability of existing pigment algorithms to Southern Ocean waters (Fig. 1A). South of 30°S, we found chl *a* + phaeo concentrations in situ averaged 0.58 mg m^{-3} (n = 6173 data elements). Fukuchi (*16*) reported, for waters between 35° and 63°S, a mean in situ pigment concentration of 0.38 mg m^{-3} for chl *a* alone, or correcting for the presence of phaeopigments (with a chl *a*:phaeo ratio of 2.57 ± 1.51 in the Southern Ocean, n = 1070), 0.53 mg m^{-3} for chl *a* + phaeo. This is within 10% of our in situ estimate. For comparison, the mean CZCS pigment concentration computed with the global processing (GP) algorithm currently in wide use (*14*) was 0.32 mg m^{-3} for chl *a* + phaeo, suggesting that previously reported CZCS pigment concentrations for the Southern Ocean based on the GP algorithm are underestimated by about 45%. This result is remarkable because it was previously suspected that high pigment values based on CZCS in the polar regions may be associated with retrieval errors resulting from low solar angles and multiple scattering effects.

The large discrepancy between earlier satellite and in situ estimates may be attributed to uncharacteristically low pigment-specific absorption and low detrital concentrations of Southern Ocean waters, particularly south of the polar front (*17*). A Southern Ocean (SO) pigment algorithm (*17*) that reflects these water characteristics has recently been developed. This algorithm made use of the radiance of light reflected off of the surface [water-leaving radiances (Lu)] at wavelengths of 441, 520, and 560 nm instead of at 441, 520, and 550 nm, the values used in the GP algorithm. The SO algorithm yields pigment concentrations that are 2.1 to 2.4 times larger than those found with the GP algorithm for Lu(441):Lu(550) ratios greater than one. At higher pigment concentrations, the GP algorithm switches to the Lu(520):Lu(550) ratio, which yields results that are not significantly different from the SO algorithm Lu(520):Lu(560) ratio (*17*). This switch has not been implemented for the SO algorithm, so values are restricted to areas with ≤3.44 mg of pigment per cubic meter. The mean summer pigment (chl *a* + phaeo) concentration computed by the SO algorithm is 0.55 mg m^{-3}, within 5% of the in situ mean reported here and within 4% of that reported by Fukuchi (*16*).

The relative frequency distribution of chl *a* + phaeo (Fig. 1) for our in situ data also exhibits substantially better agreement with satellite observations when the CZCS data are adjusted to fit the SO algorithm as opposed to when they are processed by the GP algorithm. The log-normal pigment distribution and the presence of some high pigment values (2.6% of our data set, or 162 samples, have chl *a* + phaeo values >2 mg m^{-3}) results in CZCS-derived and in

C. W. Sullivan is with the Graduate Program in Ocean Science, Hancock Institute for Marine Studies, University of Southern California, Los Angeles, CA 90089–0373. K. R. Arrigo, C. R. McClain, and J. C. Comiso are with the National Aeronautic and Space Administration Goddard Space Flight Center, Greenbelt, MD 20771. J. Firestone is with General Sciences Corporation, Laurel, MD 20707.

*Present address: Director, Office of Polar Programs, National Science Foundation, 4201 Wilson Boulevard, Arlington, VA 22230.

situ mean pigment concentrations that are substantially higher than mode concentrations. Fukuchi (*16*) had a similar percentage (2%) of in situ pigment concentrations >2 mg m^{-3}. These high pigments were found in the southernmost waters, south of 63°S, generally consistent with our observations from CZCS.

To further compare the applicability of the SO algorithm and the earlier GP algorithm to Southern Ocean waters, we spatially averaged summer CZCS pigment concentrations derived for both algorithms for each 1°-wide circumpolar band between 30° and 65°S and regressed them against similarly computed mean in situ pigment concentrations (Fig. 2A). South of 65°S, both in situ and CZCS data are relatively scarce (Fig. 2B) and resulted in poor agreement between the three sets of values at these latitudes (Fig. 2C). Therefore, they were excluded from further analysis. Both the SO and GP algorithms were able to explain 71% of the variability in the data (the regression coefficients R^2 are the same because the analyses were performed on the same in situ data with constant coefficients for the SO and GP algorithms). This is encouraging and indicates that ocean color information obtained from satellites is useful for the characterization of pigment concentrations at high southern latitudes. Moreover, the best fit slope of 0.91 obtained with the SO algorithm indicates that it was a better approximation of the in situ pigment data than was the standard GP algorithm (slope = 0.41), which was developed from only 55 bio-optical stations in waters around the United States. These results emphasize the need to develop regional algorithms in the processing of ocean color data, particularly because the next ocean color mission, carrying the Sea-Viewing Wide Field-of-View Sensor (SeaWiFS), is scheduled for launch in late 1994.

Horizontal Distribution of Phytoplankton Pigments

To emphasize the distribution of phytoplankton blooms (>1 mg of pigment per cubic meter with the GP algorithm) in the Southern Ocean, we averaged all available monthly data from spring and summer (October to March, 1978 to 1986) for which each data element was ≥1 mg m^{-3} for chl *a* + phaeo (Fig. 3A). This procedure yields a much clearer image of bloom distribution than can be obtained by simple averaging of all data (Fig. 3B). Phytoplankton blooms were not evenly distributed throughout the Southern Ocean but rather were localized primarily in three regions: (i) in shallow waters near continental margins, around islands, and over shoals; (ii) in coastal polynyas of the Antarctic sea ice zone (ASIZ); and (iii) seaward, downwind, and downstream of continental masses that interrupt the flow fields of major circumpolar currents in the sub-Antarctic zone (SAZ) and the polar front zone (PFZ) between 45° and 60°S. Blooms in shallow coastal waters and coastal polynyas have been described (*11, 18*), so we will focus on phytoplankton blooms over shelves and in deeper waters.

Because major nutrients generally are believed to be sufficient in most Southern Ocean regions south of the polar front, it has been proposed that primary productivity there is determined by the availability of iron (*19–23*) and furthermore, that the iron probably is derived from icebergs and shelf sediments (*24, 25*). For example, measurements of iron concentration ranged from 2 to 8 nM in surface waters of the Weddell Sea and Weddell Sea–Scotia Sea confluence (*24*) but were an order of magnitude greater over the South Orkney Shelf (≈60 nM), where our CZCS data revealed a major bloom (Fig. 3A). Total and dissolved iron is transported from the Filchner Shelf into the Weddell Sea basin (*25*). Surface concentrations of iron in the Weddell Gyre were 1 nM but rose considerably over the shelves. Similarly, blooms in the vicinities of the Agulhas Retroflection, the Patagonian Shelf, the Tasman Sea, and the shelf west of New Zealand were adjacent to and downflow of shelf regions (Fig. 3A). Deposition of atmospheric dust in this region is low (*26, 27*), suggesting that these regions are not fer-

A

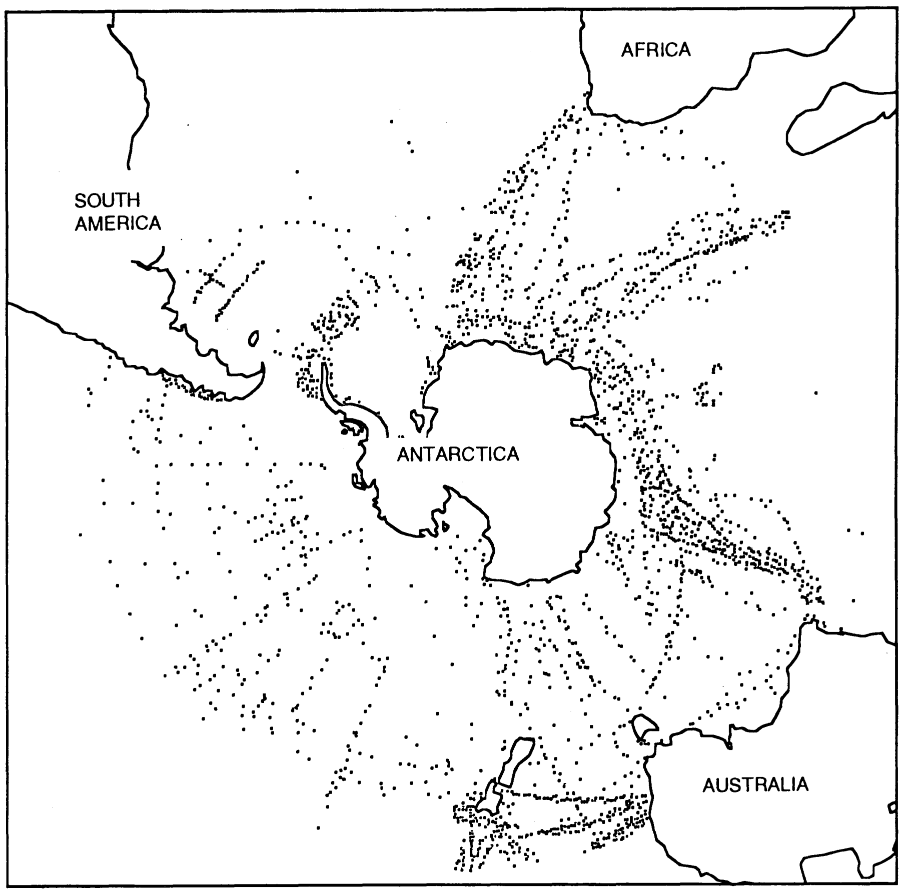

B

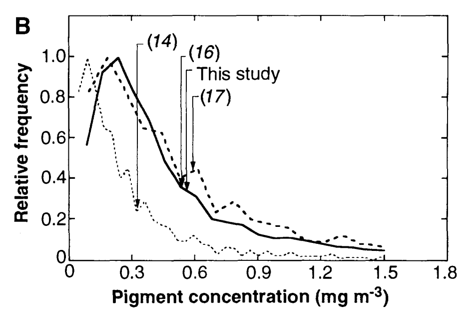

Fig. 1. (**A**) Stations where in situ pigment samples from surface waters were collected. (**B**) Relative-frequency distribution of chl *a* + phaeo for in situ data (solid line) and for the CZCS data processed by the SO algorithm (dashed line, n = 98,869) and the GP algorithm (dotted line, n = 100,607). Mean values from four studies are marked by arrows. All pigment concentrations from CZCS in excess of 10 mg m^{-3} (<1% of all samples) were excluded from the analysis because of suspected unreliability. To maintain consistency, the same was done with the in situ pigment data (10 out of 6183 data points were excluded).

tilized by aeolian input of iron-rich dust from the continents. In addition, a recent study (*12*) of satellite data revealed no evidence of strong coherence between high aerosol concentrations and areas of phytoplankton blooms. Thus, published data combined with CZCS images suggest that iron transported from shelf regions to the deep ocean may stimulate and sustain phytoplankton blooms over and downflow of the shelves (Fig. 3A).

The CZCS data show a background of low pigment levels (<0.1 mg m^{-3}) at low latitudes. An extensive circumpolar region of enhanced pigments lies south of ~30° to 35°S latitude and extends to the continent of Antarctica (Fig. 3B). The entire region of enhanced pigments (>0.1 mg m^{-3}) forms a large asymmetric pattern around the Antarctic continent, with waters in the southeast Pacific region to the west of Chile being depleted in surface pigments (<0.1 mg m^{-3}). The northern edge of enhanced pigments occurs at 30° to 35°S in the southwest Atlantic and moves south as one moves west to east (*28*), reaching only to <50°S in the southeast Pacific.

We compared the observed asymmetric distribution pattern of enhanced pigments in the Southern Ocean with the distribution of several geophysical features (*13*, *29*) to determine which among them were similarly distributed at the ocean-basin scale. The excursions in the asymmetrical pattern of pigments are downwind and downcurrent of major continental masses and appear to be a result, in part, of the nature of the Antarctic Circumpolar Current; it essentially becomes a meridional current in the southwest Atlantic in the region of the Falkland and Brazil Current (*30*, *31*) but to the east remains largely zonal through most of the south Atlantic and Indian Ocean (Fig. 4A), finally weakening in the southeast Pacific (*28*, *31*). The distribution of silicic acid (*29*) concentrations >5 μM is similarly asymmetrical (Fig. 4B). Kamykowski and Zentara (*32*) have shown the incidence of excess nitrate at silicic acid depletion in the southeast Pacific; in the region between 140° to 71°W and 30° to 60°S, up to 15 μM nitrate remained when silicic acid was depleted. The nitrate excess and silicic acid depletion would limit diatom growth in the surface waters of this region, resulting in low pigment concentrations. The low productivity of Antarctic phytoplankton may reflect factors that limit their assimilation of this essential nutrient by diatoms (*33*). The concentration-dependent uptake of silicic acid into diatoms characterizes the transport system responsible for providing silica to build the cell wall (*33*). The affinity constant for silicic acid transport in Antarctic diatoms lies between 12 and 22 μM; thus at lower concentrations, the growth rate falls off quickly (*34*). Because silicic acid concentrations of <2 μM are characteristic of much of the southeast Pacific sector (*29*, *32*) (Fig. 4B), the growth of diatoms will be severely limited there.

These observations argue strongly that a nutrient-based, or "bottom-up," control of phytoplankton production takes place in the southeast Pacific and perhaps in some broader regions of the Southern Ocean. Within the large-scale asymmetric feature of enhanced pigments, there are two extensive, nearly concentric rings or bands of pigments separated by waters with lower pigment levels between 45° and 55°S (Fig. 3). This banding pattern becomes particularly obvious when pigment is plotted as a function of latitude (Fig. 5). However, it should be noted that the patterns spiral inward somewhat, causing a broadening of each band when plotted in this way. The northern band (labeled "1" in Fig. 5) principally occupies the SAZ, which lies between the subtropical front (STF) and sub-Antarctic front (SAF) (*1*, *31*, *35*). Temperature varies from 20° to 5°C (*13*, *36*), and mean pigment concentration is 0.29 mg m^{-3}. It is the most prominent large-scale pigment feature in the Southern Ocean and diminishes only in the southeast Pacific in a fashion that gives the appearance of a circumpolar, clockwise spiral to the enhanced pigment field that characterizes the Southern Ocean (Fig. 3B). Sea surface temperature (SST) is symmetrically distributed about the Antarctic continent (*12*), indicating that temperature per se is not a major determinant of pigment distributions.

The southern band lies within the PFZ; here SSTs range from −2° to 8°C. This is the least well defined band, but it can be seen clearly south of Africa between 10° and 35°E (Fig. 3B). It is composed of three primary regions of high pigments. The first, region 2 (Fig. 5), extends from 50° to 57°S and includes blooms in the northern Scotia Sea. Region 3 includes phytoplankton blooms over the Scotia ridge, in the Bransfield Strait, and above the Pacific Antarctic Ridge. This region extends from 57° to 65°S and includes the ASIZ in the region of seasonal pack-ice melt (*10*). Here, summer SST ranges from ~3.5° to −2°C, and mean pigments, at 0.47 mg m^{-3}, are the highest observed in the open ocean away from continental borders. Region 4 lies south of 65°S and is dominated by coastal phytoplankton blooms.

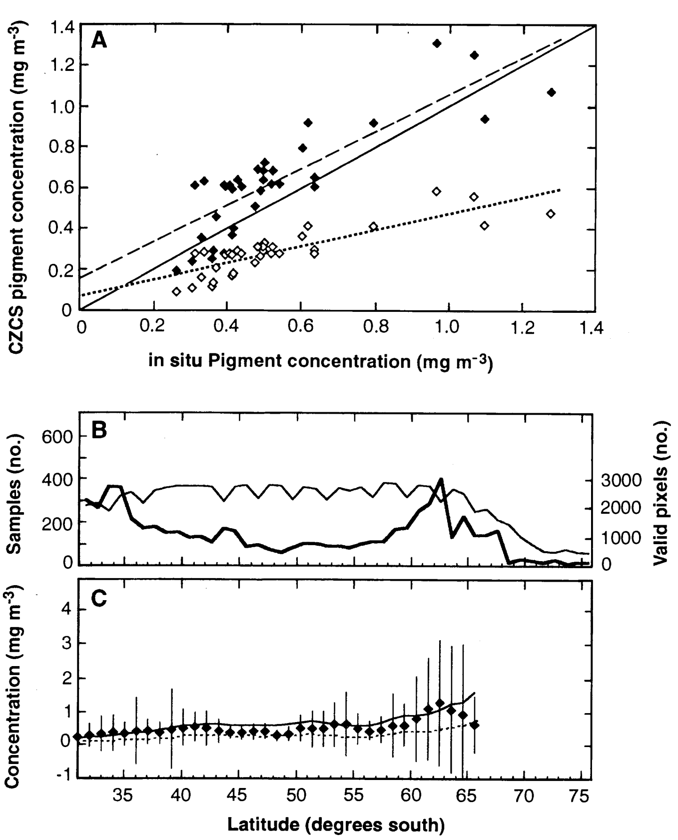

Fig. 2. (**A**) CZCS pigment (chl *a* + phaeo) concentration, estimated with the GP (open symbols) and the SO (filled symbols) (*51*) algorithms, versus in situ pigment concentration. Data points were calculated as circumglobal means for each 1° of latitude between 30° and 65°S. The solid line is the line of perfect agreement between CZCS and in situ data. The equation for the dotted line is $y = 0.07 + 0.407x$ (*14*), and that for the dashed line is $y = 0.16 + 0.905x$ (*17*). (**B**) The total number of data points for CZCS (valid pixels, thin line) and in situ (samples, heavy line) measurements for each 1° of latitude between 30° and 65°S. All analyses were performed with SEAPAK software (*52*) on a composited summer (October to March) image. (**C**) In situ (diamond) and CZCS pigment concentrations estimated with the GP (dashed line) (*14*) and the SO (solid line) (*17*) algorithms averaged for each 1° of latitude plotted versus latitude. As latitude increases, the number of valid pixels decreases. Poor agreement south of 65°S may be attributable to small sample size.

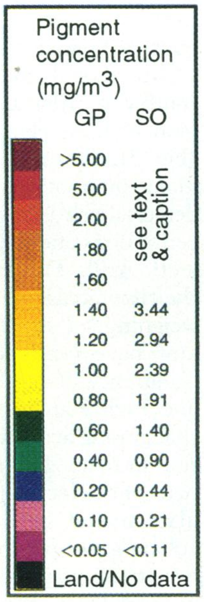

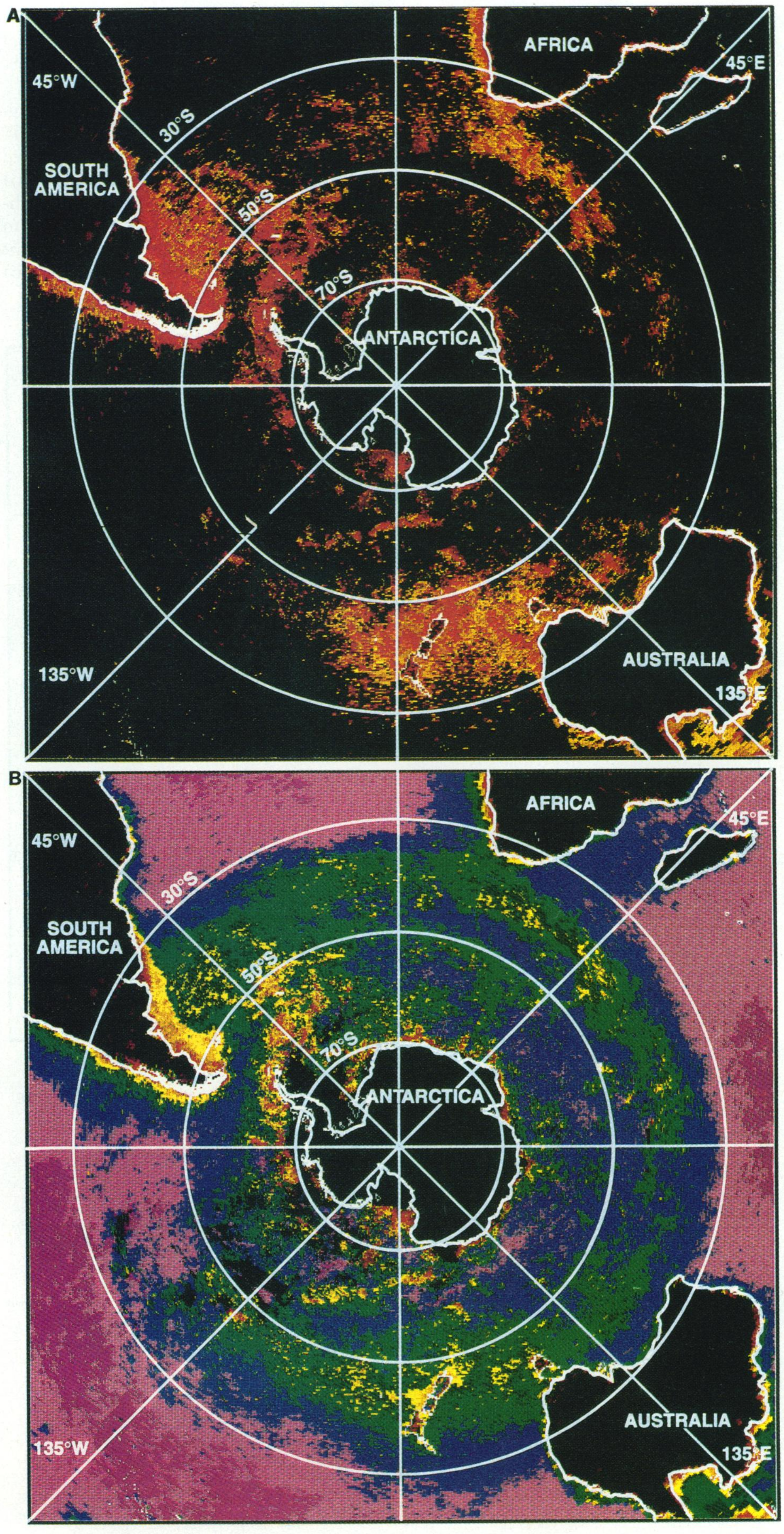

Fig. 3. (**A**) Phytoplankton blooms from mean pigment (chl *a* + phaeo) concentrations for all CZCS data >1 mg m^{-3} (on the basis of the GP algorithm) averaged monthly between November 1978 and June 1986. (**B**) Mean seasonal pigment concentrations averaged from monthly means during summer (October to March, 1978 to 1986). The scale for the SO algorithm is restricted to values ≤3.44 mg m^{-3} because at this concentration a switch from the Lu(441):Lu(560) radiance ratio to a Lu(520):Lu(560) ratio should be implemented. Unfortunately, the implementation of this switch has not been completed.

Low pigment (<0.1 mg m^{-3}) waters separate the two major bands of high pigments, appearing globally at latitudes north of 30° or 35°S, in a band south of 55°S between 45° and 170°E, and between 30° and 50°S in the southeast Indian and southeast Pacific Oceans. These enhanced pigment regions appear to correspond rather closely with the zones defined by Kamykowski and Zentara (*37*) on the basis of plant-nutrient utilization rates. The three zones they distinguished were (i) STF to the SAF, (ii) PFZ to the Antarctic Divergence, and (iii) the area south of the Antarctic Divergence (63°S to Antarctic continent).

The region of reduced pigments in the western Indian Ocean is coincident with the zonal region of high wind stress (*12*, *13*, *38*) and deep mixed layers (*39*). This particular relation between physical and biological fields is especially prominent in the southeastern Indian ocean sector but is not apparent in the Drake Passage region. A simple explanation for this relates to the inverse relation expected between high wind stress, producing deep mixed layers, and low primary production because of the low average irradiance a deeply mixed phytoplankter experiences (*40*). Under these conditions, phytoplankton are unable to carry out photosynthesis for sufficiently long periods to allow net growth. As a result, the rate of loss processes such as sinking and grazing exceed that of the growth of phytoplankton; consequently, phytoplankton do not accumulate in surface waters and blooms do not occur.

Mean summer (October to March) pigment levels (0.47 mg m^{-3}) in the ASIZ were the highest revealed by CZCS in the pelagic regions of the Southern Ocean; the mean value for blooms (>1 mg m^{-3}) in the ASIZ, 4.5 mg m^{-3}, also was the highest among the observed Southern Ocean blooms. Both observations lead to the counterintuitive conclusion that the highest phytoplankton crops occur in the coldest waters of the Southern Ocean. This observation may just be coincidental because of the favorable light environment provided by the well-known vertical stability in the ASIZ (*10–13*). Nevertheless, photoacclimation to low temperature by phytoplankton inhabiting waters south of the Antarctic Convergence has been observed (*41*).

Taken together, these observations suggest that local distributions of phytoplankton in the Southern Ocean are influenced by different chemical or physical factors: (i) low silicic acid concentrations in the southeastern Pacific; (ii) low light availability in areas of deep mixing, but a favorable light environment in stratified waters; and (iii) iron availability downstream of continents, over shallow areas, and near icebergs.

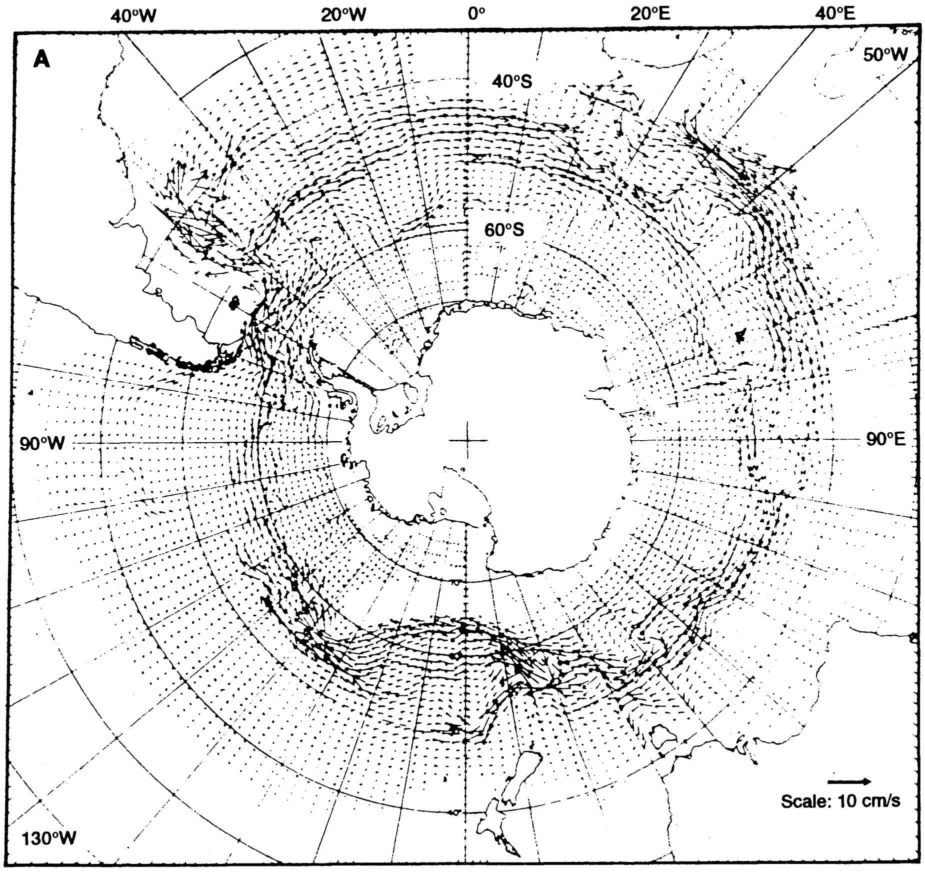

Fig. 4. (**A**) Geostrophic current at the sea surface relative to the 100-dbar level (*28*) and (**B**) surface nutrient concentration isolines for >10 μM nitrate, >1 μM phosphate, and >5 μM silicic acid in the Southern Ocean [adapted from (*29*)]. Cross-hatched regions denote areas of silicic acid limitation.

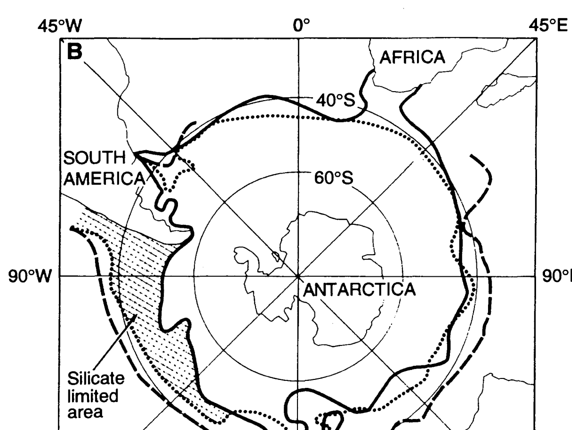

Meridional zonation is noted in the southwest Atlantic (45° to 55°W), the region of most persistent biological activity (Fig. 3). This region also is recognized as a major international fishery for ground and demersal fish (*42*) and for the highest concentrations and largest areal extent of Antarctic krill, *Euphausia superba* (Dana), in the circumpolar ocean (*43*). Swarms of krill weighing $>2 \times 10^6$ tons in an area of 450 km^2 have been described (*44*). The cooccurrence of dense phytoplankton blooms and high standing stocks of krill suggest that grazing activity and fecal pellet production in this region may be a major determinant of the locus of intense fluxes of particulate matter to the ocean interior. The coherence of phytoplankton and zooplankton stocks may argue for grazer-dominated or "top-down" regulation of production in localized areas. It has been reported that silica-containing diatoms dominate the downward flux of particulate matter as evidenced by the rich siliceous oozes that characterize sediments in the region (*43–47*). Thus, phytoplankton distributions at the planetary scale are predictive of distributions of living marine resources and associated biogeochemical processes.

We have shown that satellite-derived pigment distributions can be a useful resource to guide and focus future field programs and modeling studies that address the role of the Southern Ocean in the contemporary cycle of carbon in the sea and the coupled oceanic processes regulating atmospheric carbon dioxide concentrations. They also may be used to gain insight into potential sites of enhanced flux of particulate matter to the deep ocean (*45, 46*), the nature and extent of deposits of siliceous sediments (*45*), as well as likely locations of concentrations of marine living resources, including krill (*43*), fish (*42*), marine mammals (*48*), and birds (*49, 50*). Identification of the geographical extent and magnitude of persistent blooms enables both a qualitative and

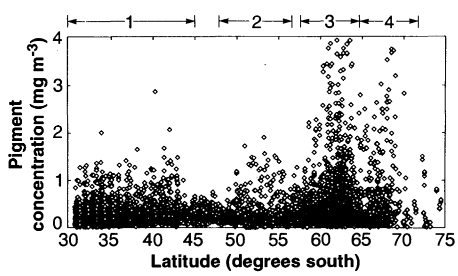

Fig. 5. Scatter plot of in situ pigment (chl *a* + phaeo) concentration versus latitude (*n* = 6183). Eighty-six data points for which the concentration was >3 mg m^{-3} are not shown.

quantitative evaluation of the role of phytoplankton and biological productivity in ecological, biogeochemical, and climatological investigations of the region.

REFERENCES AND NOTES

1. W. D. Nowlin Jr. and J. M. Klinck, *Rev. Geophys.* **24**, 469 (1986).
2. J. L. Sarmiento and J. R. Toggweiler, *Nature* **308**, 621 (1984).
3. T. H. Peng *et al.*, *Tellus Ser. B* **39**, 439 (1987).
4. J. L. Sarmiento *et al.*, *Philos. Trans. R. Soc. London Ser. A* **325**, 3 (1988).
5. M. J. R. Fasham *et al.*, *J. Mar. Res.* **48**, 591 (1990).
6. L. Labeyrie *et al.*, paper presented at the International Symposium on Biogeochemistry and Circulation of Water Masses in the Southern Ocean, Brest, France, 2 to 6 July 1990.
7. L. Legendre *et al.*, *Polar Biol.* **12**, 429 (1992).
8. T. Platt and S. Sathyendranath, *Science* **241**, 1613 (1988).
9. B. Frost, *Limnol. Oceanogr.* **36**, 1616 (1991).
10. C. W. Sullivan *et al.*, *J. Geophys. Res.* **93**, 12487 (1988).
11. J. C. Comiso *et al.*, *ibid.* **95**, 9481 (1990).
12. J. C. Comiso *et al.*, *ibid.* **98**, 2419 (1993).
13. C. R. McClain *et al.*, *Eos* **72**, 345 (1991).
14. H. R. Gordon *et al.*, *Appl. Opt.* **22**, 20 (1983).
15. W. M. Balch *et al.*, *J. Geophys. Res.* **97**, 2279 (1992).
16. M. Fukuchi, *Oceanogr. Soc. Jpn. J.* **36**, 73 (1980).
17. B. G. Mitchell and O. Holm-Hansen, *Deep-Sea Res.* **38**, 1009 (1991); B. G. Mitchell, *J. Mar. Syst.* **3**, 91 (1992). Because of differences between the wavelength of the denominator (550 versus 560 nm), the SO algorithm will differ from the GP with the spectral radiance ratios being up to 15% less for high-pigment waters and 15% less for low pigment waters. A serious calibration error by the manufacturer of the optical equipment used to collect data for the SO algorithm resulted in absolute radiance errors of up to a factor of 2. However, for the wavelength ratios used in the SO algorithm, most of the errors canceled in the wavelength ratios. On the basis of a recent rigorous intercalibration sponsored by the National Aeronautics and Space Administration (NASA), the residual errors for the SO algorithm that we could not compensate for by taking ratios resulted in an underestimate of 5% and 10% for the Lu(441):Lu(560) and Lu(520):Lu(560), respectively (B. G. Mitchell, personal communication).
18. O. Holm-Hansen and B. G. Mitchell, *Deep-Sea Res.* **38**, 961 (1991).
19. H. J. W. de Baar *et al.*, *Mar. Ecol. Prog. Ser.* **65**, 105 (1990).
20. J. H. Martin, R. M. Gordon, S. E. Fitzwater, *Nature* **345**, 156 (1990).
21. J. H. Martin *et al.*, *Global Biogeochem. Cycles* **4**, 5 (1990).
22. A. G. J. Buma *et al.*, *Limnol. Oceanogr.* **36**, 1865 (1991).
23. J. H. Martin *et al.*, *ibid.*, p. 1793.
24. R. F. Nolting *et al.*, *Mar. Chem.* **35**, 219 (1991).
25. E. Westerlund and P. Ohman, *ibid.*, p. 199.
26. R. Deuce *et al.*, in *The Role of Air-Sea Exchange in Geochemical Cycling*, P. Buat-Menard, Ed. (Reidel, Dordrecht, Netherlands, 1986), pp. 497–529.
27. R. Deuce and N. W. Tindale, *Limnol. Oceanogr.* **36**, 1715 (1991).
28. A. L. Gordon *et al.*, *J. Geophys. Res.* **83**, 3023 (1978).
29. A. L. Gordon *et al.*, Ed., *Southern Ocean Atlas* (Columbia Univ. Press, New York, 1986).
30. R. G. Peterson and T. Whitworth III, *J. Geophys. Res.* **94**, 10817 (1989).
31. E. E. Hofmann, **90**, 7087 (1985).
32. D. Kamykowski and S. J. Zentara, *Deep-Sea Res.* **28**, 455 (1981).
33. C. W. Sullivan, in *Silicon Biochemistry*, D. Evered and M. O'Connor, Eds. (CIBA Foundation Symposium 121, WIley, Chichester, United Kingdom, 1986), pp. 59–89.
34. G. Jacques, *Polar Biol.* **2**, 27 (1983).
35. M. A. Clifford, thesis, Texas A&M University, College Station (1982).
36. R. W. Reynolds, *J. Clim.* **1**, 75 (1988).
37. D. Kamykowski and S. J. Zentara, *Mar. Ecol. Prog. Ser.* **58**, 101 (1989).
38. K. E. Trenberth *et al.*, *J. Phys. Oceanogr.* **20**, 1742 (1990).
39. S. Levitus, *NOAA* (*Natl. Oceanic Atmos. Admin.*) *Prof. Pap. 13* (1982).
40. B. G. Mitchell *et al.*, *Limnol. Oceanogr.* **38**, 1662 (1991).
41. M. M. Tilzer *et al.*, *Polar Biol.* **5**, 105 (1986).
42. T. G. Lubimova, selected papers presented to Scientific Committee of Committee for Conservation of Antarctic Marine Living Resources 1982–1984 (1985), vol. 1, p. 329.
43. R. M. Laws, *Am. Sci.* **73**, 26 (1985).
44. J. P. Croxall, in *Antarctic Ecology*, R. M. Laws, Ed. (Academic Press, New York, 1984), vol. 2, pp. 533–621.
45. G. Wefer and G. Fischer, *Mar. Chem.* **35**, 597 (1991).
46. D. J. DeMasters *et al.*, *ibid.*, p. 489.
47. D. J. DeMasters, *Geochim. Cosmochim. Acta* **45**, 1715 (1981).
48. R. M. Laws, in (*44*), pp. 621–717.
49. J. Croxall *et al.*, in *Antarctic Ocean and Resources Variability*, D. Sarhage, Ed. (Springer-Verlag, New York, 1988), p. 261.
50. W. Trivelpiece *et al.*, in *Antarctic Ecosystems: Ecological Change and Conservation*, K. R. Kerry and G. Hempel, Eds. (Springer-Verlag, New York, 1990), pp. 191–202.
51. We approximated the output of the SO algorithm by applying a conversion factor computed for each pigment interval (0.05 mg m^{-3} for chl a + phaeo) to the standard CZCS output (computed from the GP algorithm) using the appropriate Lu ratio given below. Pigment algorithms: log(chl a + phaeo) = a + $b$log[Lu(441)/Lu(550)] for chl $a < 1.5$ mg m^{-3} and log(chl a + phaeo) = a + $b$log[Lu(520)/Lu(550)] for chl $a > 1.5$ mg m^{-3}. The constants are, for the GP Lu(441)/Lu(550) algorithm, $a = 0.14$ and $b = 1.55$; for the SO Lu(441)/Lu(550) algorithm, $a = 0.53$ and $b = 1.63$; for the GP Lu(520)/Lu(550) algorithm, $a = 0.63$ and $b = 4.72$; and for the SO Lu(520)/Lu(550) algorithm, $a = 0.48$ and $b = 3.32$. There is no statistical difference between the GP and the SO Lu(520)/Lu(550) algorithms.
52. C. R. McClain *et al.*, "SEAPAK User's Guide," *NASA TM 100728* (1991).

53. We thank J. Campbell, C. Fritsen, D. A. Kiefer, and C. Mordy for comments on earlier versions of this manuscript. In situ pigment data were provided by G. Mitchell, D. Biggs, S. El-Sayed, J. Bradford, W. Smith, E. Sakshaug, O. Holm-Hansen, the British Antarctic Survey (J. Priddle), the Japanese Antarctic Research Expeditions (M. Fukuchi), S. Wright, and the Alfred-Wegener-Institute für Polar- und Meeresforschung (G. Dieckmann). This work was supported by grants from the National Science Foundation, Division of Polar Programs (C.W.S.), and the National Aeronautics and Space Administration (C.R.M. and J.C.C.) and by a U.S. Department of Energy Global Change Distinguished Postdoctoral Fellowship (K.R.A.) administered by the Oak Ridge Institute for Science and Education.